Advances in Applied Mathematics and Mechanics
Adv. Appl. Math. Mech., Vol. **8**, No. 6, pp. 911-931

DOI: 10.4208/aamm.2015.m1065
December 2016

Moving Finite Element Methods for a System of Semi-Linear Fractional Diffusion Equations

Jingtang Ma* and Zhiqiang Zhou

School of Economic Mathematics, Southwestern University of Finance and Economics, Chengdu 611130, China

Received 26 April 2015; Accepted (in revised version) 17 November 2015

Abstract. This paper studies a system of semi-linear fractional diffusion equations which arise in competitive predator-prey models by replacing the second-order derivatives in the spatial variables with fractional derivatives of order less than two. Moving finite element methods are proposed to solve the system of fractional diffusion equations and the convergence rates of the methods are proved. Numerical examples are carried out to confirm the theoretical findings. Some applications in anomalous diffusive Lotka-Volterra and Michaelis-Menten-Holling predator-prey models are studied.

AMS subject classifications: 65M60, 65M12, 65M06, 35S10, 65R20

Key words: Finite element methods, fractional differential equations, predator-prey models.

1 Introduction

In this paper, we consider a system of semi-linear fractional diffusion equations of the following form

$$u_t - \mathscr{D}_1 \frac{\partial^{2-\beta_1} u}{\partial x^{2-\beta_1}} = f_1(u,v) + h_1(x,t), \tag{1.1a}$$

$$v_t - \mathscr{D}_2 \frac{\partial^{2-\beta_2} v}{\partial x^{2-\beta_2}} = f_2(u,v) + h_2(x,t), \tag{1.1b}$$

$$u(x,0) = \varphi(x), \qquad u(a,t) = u(b,t) = 0, \tag{1.1c}$$

$$v(x,0) = \psi(x), \qquad v(a,t) = v(b,t) = 0, \tag{1.1d}$$

for $(x,t) \in \Omega \times \mathbb{T}$ with $\Omega = (a,b)$, $\mathbb{T} = (0,T)$, where the functions f_i and h_i, positive constants $\mathscr{D}_i$ for $i=1,2$, and φ, ψ are given, and assume that f_i $(i=1,2)$ satisfy the following mixed local Lipschitz conditions

$$|f_i(u_1,u_2) - f_i(v_1,v_2)| \le L(|u_1 - v_1| + |u_2 - v_2|), \quad i=1,2, \tag{1.2}$$

*Corresponding author.
Email: mjt@swufe.edu.cn (J. T. Ma), zqzhou@2014.swufe.edu.cn (Z. Q. Zhou)

for all u_1, u_2, v_1, $v_2 \in \Theta \subset \mathbb{R}$, where L is positive constant, and the space fractional derivatives are defined by

$$\frac{\partial^{2-\beta_i} u(x,t)}{\partial x^{2-\beta_i}} = D[p\,{}_aD_x^{-\beta_i} + q\,{}_xD_b^{-\beta_i}]Du(x,t), \tag{1.3}$$

where D denotes a single partial derivative, ${}_aD_x^{-\beta_i}$ and ${}_xD_b^{-\beta_i}$ represent left and right Riemann-Liouville fractional integral operators, $0<\beta_i<1$ $(i=1,2)$, p and q are two constants satisfying that $0\le p,q\le 1$, $p+q=1$.

The above model has many applications in population growth modeling (see e.g., [1, 2, 4, 5, 26]). Baeumer et al. [1, 2] studied the anomalous diffusion (fractional diffusion) population growth model for single specie. For competitive predator-prey models, the standard second-order diffusion models have been well studied (see e.g., [4, 5, 26]); however the studies on anomalous diffusion models are not many in the literature (we are only aware that Yu, Deng and Wu [47] studied the finite difference methods for the competitive predator-prey models with anomalous diffusion).

More specifically, the anomalous diffusion (fractional diffusion) predator-prey models studied in this paper include Lotka-Volterra and Michaelis-Menten-Holling types. Let u and v denote the population densities of prey and predator, respectively, $\mathscr{D}_i$ $(i=1,2)$ the coefficients of dispersion. If $h_i(x,t)\equiv 0$ for $i=1,2$, then the system is closed, i.e., u and v will develop freely, without influence from outside.

The competitive Lotka-Volterra models are described as follows. Let

$$f_1(u,v) = r_1 u\Big(1-\frac{a_{11}u+a_{12}v}{K_1}\Big), \tag{1.4a}$$

$$f_2(u,v) = r_2 v\Big(1-\frac{a_{22}v+a_{21}u}{K_2}\Big), \tag{1.4b}$$

where constants r_1, r_2 are inherent per-capita growth rates, constants K_1, K_2 are the carrying capacities, constants constants a_{12}, a_{21} represent the effect of the two species on each other, constants a_{11}, a_{22} are self-interacting factors for the two species. Then system (1.1a)-(1.1b) with (1.4a) and (1.4b) characterizes the well-known competitive Lotka-Volterra models (see e.g., [4]).

The Michaelis-Menten-Holling predator-prey model is a kind of ratio-dependent type predator-prey models. It is characterized by system (1.1a)-(1.1b) with the following Michaelis-Menten type functional response

$$f_1(u,v) = ru\Big(1-\frac{u}{K}-\frac{d_1 v}{\kappa v+u}\Big), \tag{1.5a}$$

$$f_2(u,v) = v\Big(-Q(v)+\frac{d_2 u}{\kappa v+u}\Big), \tag{1.5b}$$

where d_1, d_2, κ, K, and r are positive constants. Here, $Q(v)$ denotes a mortality function of predator, and r and K the prey growth rate with intrinsic growth rate and the carrying capacity in the absence of predation, respectively, while d_1, d_2, and κ are model-dependent constants. The Michaelis-Menten-Holling predator-prey model was first introduced and intensively studied by Cavani and Farkas [5], where they analyzed the existence result and stability of pattern formations. Kovács et al. [26] have achieved a qualitative behavior of the ratio-dependent predator-prey system.

In this paper, we propose a moving finite element method to solve a system of fractional differential equations arising in the anomalous diffusion predator-prey models. We extend the convergence analysis of moving mesh finite element methods for linear single fractional differential equation in Ma et al. [34] to a system of two semi-linear fractional differential equations and apply the methods to the anomalous diffusion predator-prey models.

To be more instructive, we give a brief review of the numerical methods for fractional differential equations. In the history, the numerical methods on fixed mesh for fractional differential equations have been received a lot of studies (see e.g., [6–8, 10, 18, 19, 21–23, 37, 38, 40–43, 46, 48, 51, 52], which focus on finite difference methods; [9, 13–17, 24, 27, 28, 36, 39, 49, 50] on Galerkin methods or finite element methods.) However, there are not many references on developing moving mesh methods for fractional differential equations. Ma and Jiang [33] developed moving mesh collocation methods to solve nonlinear time fractional partial differential equations with blowup solutions; however the analysis was not provided by the paper. Although moving mesh methods have been well developed (see e.g., the books [20, 44]), the convergence analyses have not been fully understood, hitherto having only focused on integer differential equations (see e.g., [3, 11, 12, 29–32, 35]). Jiang and Ma [25] analyzed moving mesh finite element methods for a linear single time fractional partial differential equation.

The remaining parts of the paper are arranged as follows. In Section 2, the moving finite element methods are introduced and the convergence rates are analyzed. In Section 3, a variety of numerical examples are provided to verify the convergence rates and applications in the predator-prey models are given. In the final section, conclusions are provided.

Throughout the paper, we use notation $g_1 \lesssim g_2$ and $g_1 \gtrsim g_2$ to denote $g_1 \leq Cg_2$ and $g_1 \geq Cg_2$, respectively, where C is a generic positive constant independent of any functions and numerical discretization parameters.

2 Moving finite element methods and convergence analysis

Define left Riemann-Liouville fractional integral as

$$ {}_aD_x^{-\sigma}u(x)=\frac{1}{\Gamma(\sigma)}\int_a^x (x-\xi)^{\sigma-1}u(\xi)d\xi, \quad x>a, \quad \sigma>0, \tag{2.1}$$

where $a\in\mathbb{R}$ or $a=-\infty$, and right Riemann-Liouville fractional integral as

$$ {}_xD_b^{-\sigma}u(x)=\frac{1}{\Gamma(\sigma)}\int_x^b (\xi-x)^{\sigma-1}u(\xi)d\xi, \quad x<b, \quad \sigma>0, \tag{2.2}$$

where $b\in\mathbb{R}$ or $b=+\infty$. The Caputo left and right fractional derivatives are defined by, respectively,

$$
\begin{aligned}
{}_aD_x^{\mu}u(x) &= {}_aD_x^{-\sigma}D^n u(x), &\quad \sigma &= n-\mu, &\quad n-1 &\le \mu < n, &\quad (2.3\text{a})\\
{}_xD_b^{\mu}u(x) &= {}_xD_b^{-\sigma}D^n u(x), &\quad \sigma &= n-\mu, &\quad n-1 &\le \mu < n. &\quad (2.3\text{b})
\end{aligned}
$$

Define three functional spaces $J^{\mu}_{L,0}(\Omega)$, $J^{\mu}_{R,0}(\Omega)$, $H^{\mu}_0(\Omega)$, $\mu>0$ as the closures of $C_0^{\infty}(\Omega)$ under the respective norms

$$\|u\|_{J_L^{\mu}(\Omega)} := \big(\|u\|^2_{L^2(\Omega)} + \|{}_aD_x^{\mu}u\|^2_{L^2(\Omega)}\big)^{1/2}, \tag{2.4a}$$

$$\|u\|_{J_R^{\mu}(\Omega)} := \big(\|u\|^2_{L^2(\Omega)} + \|{}_xD_b^{\mu}u\|^2_{L^2(\Omega)}\big)^{1/2}, \tag{2.4b}$$

$$\|u\|_{H^{\mu}(\Omega)} := \big(\|u\|^2_{L^2(\Omega)} + \||\omega|^{\mu}\mathcal{F}(\widehat{u})\|^2_{L^2(\mathbb{R})}\big)^{1/2}, \tag{2.4c}$$

where $\mathcal{F}(\widehat{u})$ denotes the Fourier transform of $\widehat{u}$, $\widehat{u}$ is the extension of u by zero outside of Ω.

Define a bilinear form, for $i=1,2$,

$$
\begin{aligned}
B_i(u,w) :&= p\Big\langle {}_aD_x^{-\beta_i}Du, Dw\Big\rangle + q\Big\langle {}_xD_b^{-\beta_i}Du, Dw\Big\rangle\\
&= p\Big\langle {}_aD_x^{-\beta_i/2}Du, {}_xD_b^{-\beta_i/2}Dw\Big\rangle + q\Big\langle {}_xD_b^{-\beta_i/2}Du, {}_aD_x^{-\beta_i/2}Dw\Big\rangle\\
&= p\Big\langle {}_aD_x^{\alpha_i}u, {}_xD_b^{\alpha_i}w\Big\rangle + q\Big\langle {}_xD_b^{\alpha_i}u, {}_aD_x^{\alpha_i}w\Big\rangle,
\end{aligned} \tag{2.5}
$$

where $\langle\cdot,\cdot\rangle$ denotes the duality pairing of $H^{-\alpha_i}(\Omega)$ and $H_0^{\alpha_i}(\Omega)$, $\alpha_i:=1-\beta_i/2$ $(i=1,2)$, the derivation of the last two identities can be seen from [13]. The bilinear form $B_i(\cdot,\cdot)$ satisfies the following coercive and continuous properties over space $H_0^{\alpha_i}(\Omega)$ (see e.g., [13]), for $i=1,2$,

$$
\begin{aligned}
B_i(u,u) &\gtrsim \|u\|^2_{H^{\alpha_i}(\Omega)}, &\quad \forall u &\in H_0^{\alpha_i}(\Omega), &\quad (2.6\text{a})\\
|B_i(u,v)| &\lesssim \|u\|_{H^{\alpha_i}(\Omega)}\|v\|_{H^{\alpha_i}(\Omega)}, &\quad \forall u,v &\in H_0^{\alpha_i}(\Omega). &\quad (2.6\text{b})
\end{aligned}
$$

The variational form for the system (1.1a)-(1.1b) with conditions (1.1c) and (1.1d) is defined as: Find $u\in H_0^{\alpha_1}(\Omega)$ and $v\in H_0^{\alpha_2}(\Omega)$ such that

$$
\begin{aligned}
(u_t,w) + \mathscr{D}_1B_1(u,w) &= (f_1(u,v),w) + (h_1(x,t),w), &\quad \forall w &\in H_0^{\alpha_1}(\Omega), &\quad (2.7\text{a})\\
(v_t,w) + \mathscr{D}_2B_2(v,w) &= (f_2(u,v),w) + (h_2(x,t),w), &\quad \forall w &\in H_0^{\alpha_2}(\Omega), &\quad (2.7\text{b})\\
(u(x,0),w) &= (\varphi(x),w), &\quad \forall w &\in H_0^{\alpha_1}(\Omega), &\quad (2.7\text{c})\\
(v(x,0),w) &= (\psi(x),w), &\quad \forall w &\in H_0^{\alpha_2}(\Omega), &\quad (2.7\text{d})
\end{aligned}
$$

where $(\cdot,\cdot)$ denotes L^2 inner product.

Define a temporal mesh

$$0\equiv t_0 < t_1 < \cdots < t_M \equiv T$$

and

$$\Delta t_n := t_n - t_{n-1}, \quad n = 1, \cdots, M.$$

Define spatial mesh (moving mesh) at time t_n, $n=0,1,\cdots,M$,

$$0 \equiv x_0^n < x_1^n < \cdots < x_N^n \equiv 1, \quad n = 0,1,\cdots,M,$$

and

$$\Omega_k^n := (x_{k-1}^n, x_k^n), \quad h_k^n := x_k^n - x_{k-1}^n, \quad k = 1,\cdots,N.$$

Define finite element spaces $\mathcal{V}_i^n \subset H_0^{\alpha_i}(\Omega)$ for $i=1,2$, on the above moving mesh as

$$\mathcal{V}_i^n := \Big\{ v \in H_0^{\alpha_i}(\Omega) \cap C^0(\Omega) : v|_{[x_{k-1}^n, x_k^n]} \in P_{m-1} \Big\},$$

where P_{m-1} denotes the space of polynomials of degree less than or equal to $m-1$.

Then the moving finite element method for the proposed problems is defined as: Find $U^n \in \mathcal{V}_1^n \subset H_0^{\alpha_1}(\Omega)$, $V^n \in \mathcal{V}_2^n \subset H_0^{\alpha_2}(\Omega)$, for $n=1,\cdots,M$, such that

$$\Big(\frac{U^n - \widetilde{U}^{n-1}}{\Delta t_n}, w\Big) + \mathscr{D}_1 B_1(U^n, w) = (f_1(U^n, V^n), w) + (h_1(x,t_n), w), \qquad \forall w \in \mathcal{V}_1^n, \tag{2.8a}$$

$$\Big(\frac{V^n - \widetilde{V}^{n-1}}{\Delta t_n}, w\Big) + \mathscr{D}_2 B_2(V^n, w) = (f_2(U^n, V^n), w) + (h_2(x,t_n), w), \qquad \forall w \in \mathcal{V}_2^n, \tag{2.8b}$$

$$(U^0, w) = (\varphi(x), w), \qquad \forall w \in \mathcal{V}_1^0, \tag{2.8c}$$

$$(V^0, w) = (\psi(x), w), \qquad \forall w \in \mathcal{V}_2^0, \tag{2.8d}$$

where $\widetilde{U}^{n-1} \in \mathcal{V}_1^n$ is the projection of U^{n-1} from $\mathcal{V}_1^{n-1}$ to $\mathcal{V}_1^n$, $\widetilde{V}^{n-1} \in \mathcal{V}_2^n$ is the projection of V^{n-1} from $\mathcal{V}_2^{n-1}$ to $\mathcal{V}_2^n$, which are defined by

$$(\widetilde{U}^{n-1}, w) = (U^{n-1}, w), \qquad \forall w \in \mathcal{V}_1^n, \tag{2.9a}$$

$$(\widetilde{V}^{n-1}, w) = (V^{n-1}, w), \qquad \forall w \in \mathcal{V}_2^n. \tag{2.9b}$$

To do the convergence analysis, we borrow from [34] the fractional Ritz projection operator, for $i=1,2$,

$$R_n^i : H_0^{\alpha_i}(\Omega) \longrightarrow \mathcal{V}_i^n$$

defined via, for $u \in H_0^{\alpha_i}(\Omega)$,

$$B_i(u - R_n^i u, w) = 0, \quad \forall w \in \mathcal{V}_i^n. \tag{2.10}$$

For the equi-distribution principle moving mesh defined by [34], assuming $u \in H_0^{\alpha_i}(\Omega) \cap H^{\gamma_i}(\Omega)$ $(\alpha_i \le \gamma_i \le m)$, we have the following estimation for the fractional Ritz projection operator defined by (2.10)

$$\|u - R_n^i u\|_{L^2(\Omega)} \lesssim N^{-\gamma_i} \|u\|_{H^{\gamma_i}(\Omega)}, \tag{2.11}$$

see [34] for the proof.

We shall use the following Gronwall-inequality.

Lemma 2.1. *Let $\Delta t_n>0$ and ξ_n, ρ_n, $\chi_n\geq 0$, for $1\leq n\leq m$, with $\rho_n\Delta t_n\leq 1/2$ and $\rho=\max_n\rho_n$. Then, if*

$$(1-\rho_n\Delta t_n)\chi_n\leq \Delta t_n\xi_n+(1+\rho_n\Delta t_n)\chi_{n-1},$$

there exists a positive constant C_m such that

$$\max_{0\leq n\leq m}\chi_n\leq C_m\Big\{\chi_0+\sum_{n=1}^m\xi_n\Delta t_n\Big\},$$

where

$$C_m=\prod_{n=1}^m\frac{1+\rho_n\Delta t_n}{1-\rho_n\Delta t_n}\leq C\exp\Big(c\sum_{n=1}^m\rho_n\Delta t_n\Big)\leq C\exp(c\rho T),$$

where c and C are some positive constants.

Proof. The proof is provided by Bank and Santos [3]. $\square$

Theorem 2.1. *For problem* (1.1a)-(1.1d) *with solutions $u\in H_0^{\alpha_1}(\Omega)\cap H^{\gamma_1}(\Omega)$ $(\alpha_1\leq\gamma_1)$ and $v\in H_0^{\alpha_2}(\Omega)\cap H^{\gamma_2}(\Omega)$ $(\alpha_2\leq\gamma_2)$, the moving finite element methods* (2.8c)-(2.8d) *have the following error estimation: for $m=1,\cdots,M$,*

$$\begin{aligned}&\|u(\cdot,t_m)-U^m\|_{L^2(\Omega)}+\|v(\cdot,t_m)-V^m\|_{L^2(\Omega)}\\ \lesssim&N^{-\gamma_1}\Big[\|\varphi\|_{H^{\gamma_1}(\Omega)}+\|u\|_{H^{\gamma_1}(\Omega)}+\int_0^{t_m}\|u_t\|_{H^{\gamma_1}(\Omega)}dt+\sum_{n=1}^{m+1}\|u(\cdot,t_{n-1})\|_{H^{\gamma_1}(\Omega)}\Big]\\ &+N^{-\gamma_2}\Big[\|\psi\|_{H^{\gamma_2}(\Omega)}+\|v\|_{H^{\gamma_2}(\Omega)}+\int_0^{t_m}\|v_t\|_{H^{\gamma_2}(\Omega)}dt+\sum_{n=1}^{m+1}\|v(\cdot,t_{n-1})\|_{H^{\gamma_2}(\Omega)}\Big]\\ &+\tau_m\sum_{n=1}^m\Delta t_n\big[\|u_{tt}(\cdot,t_n)\|_{L^2(\Omega)}+\|v_{tt}(\cdot,t_n)\|_{L^2(\Omega)}\big].\end{aligned}$$

Here N is the number of the spatial mesh points and $\tau_m:=\max_{0\leq n\leq m}\{\Delta t_n\}$ is the time mesh size and satisfies $L\tau_m\leq 1/2$ where L is the Lipschitz constant in (1.2).

Proof. Define the local truncation errors as

$$\begin{aligned}\mathcal{T}_1^n(x)=\frac{u(x,t_n)-u(x,t_{n-1})}{\Delta t_n}-u_t(x,t_n),\\ \mathcal{T}_2^n(x)=\frac{v(x,t_n)-v(x,t_{n-1})}{\Delta t_n}-v_t(x,t_n),\end{aligned}$$

where $u(x,t)$ and $v(x,t)$ are the exact solutions of (1.1a)-(1.1d). Moreover, we have the identity

$$\begin{aligned}
&\Big(\frac{u(\cdot,t_n)-u(\cdot,t_{n-1})}{\Delta t_n},w\Big)+\mathscr{D}_1B_1(u(\cdot,t_n),w)\\
&=(f_1(u(\cdot,t_n),v(\cdot,t_n)),w)+(h_1(x,t_n),w)+(\mathcal{T}_1^n,w),\quad \forall w\in\mathcal{V}_1^n, &(2.12a)\\
&\Big(\frac{v(\cdot,t_n)-v(\cdot,t_{n-1})}{\Delta t_n},w\Big)+\mathscr{D}_2B_2(v(\cdot,t_n),w)\\
&=(f_2(u(\cdot,t_n),v(\cdot,t_n)),w)+(h_2(x,t_n),w)+(\mathcal{T}_2^n,w),\quad \forall w\in\mathcal{V}_2^n. &(2.12b)
\end{aligned}$$

Let

$$\begin{aligned}
&e_1^n=u(\cdot,t_n)-U^n, &&\widetilde{e}_1^n=u(\cdot,t_n)-\widetilde{U}^n,\\
&e_2^n=v(\cdot,t_n)-V^n, &&\widetilde{e}_2^n=v(\cdot,t_n)-\widetilde{V}^n.
\end{aligned}$$

Then subtracting (2.8a) by (2.12a) and subtracting (2.8b) by (2.12b) give the error equations

$$\begin{aligned}
&\Big(\frac{e_1^n-\widetilde{e}_1^{n-1}}{\Delta t_n},w\Big)+\mathscr{D}_1B_1(e_1^n,w)\\
&=\big(f_1(u(\cdot,t_n),v(\cdot,t_n))-f_1(U^n,V^n),w\big)+(\mathcal{T}_1^n,w),\qquad \forall w\in\mathcal{V}_1^n, &(2.13a)\\
&\Big(\frac{e_2^n-\widetilde{e}_2^{n-1}}{\Delta t_n},w\Big)+\mathscr{D}_2B_2(e_2^n,w)\\
&=\big(f_2(u(\cdot,t_n),v(\cdot,t_n))-f_2(U^n,V^n),w\big)+(\mathcal{T}_2^n,w),\qquad \forall w\in\mathcal{V}_2^n. &(2.13b)
\end{aligned}$$

Define

$$\begin{aligned}
&\sigma_1^n:=R_n^1u(\cdot,t_n)-U^n, &&\epsilon_1^n:=R_n^1u(\cdot,t_n)-u(\cdot,t_n),\\
&\sigma_2^n:=R_n^2v(\cdot,t_n)-V^n, &&\epsilon_2^n:=R_n^2v(\cdot,t_n)-v(\cdot,t_n),
\end{aligned}$$

where R_n^i $(i=1,2)$ are the fractional Ritz projection operators defined by (2.10). Then

$$e_i^n=\sigma_i^n-\epsilon_i^n,\quad i=1,2.$$

Using (2.10), we re-write the error equations (2.13a) and (2.13b) as

$$\begin{aligned}
&(\sigma_1^n,w)+\mathscr{D}_1\Delta t_nB_1(\sigma_1^n,w)\\
&=(\epsilon_1^n-\epsilon_1^{n-1},w)+(\sigma_1^{n-1},w)-(e_1^{n-1}-\widetilde{e}_1^{n-1},w)\\
&\qquad+\Delta t_n\big(f_1(u(\cdot,t_n),v(\cdot,t_n))-f_1(U^n,V^n),w\big)+\Delta t_n(\mathcal{T}_1^n,w),\quad \forall w\in\mathcal{V}_1^n, &(2.14a)\\
&(\sigma_2^n,w)+\mathscr{D}_2\Delta t_nB_2(\sigma_2^n,w)\\
&=(\epsilon_2^n-\epsilon_2^{n-1},w)+(\sigma_2^{n-1},w)-(e_2^{n-1}-\widetilde{e}_2^{n-1},w)\\
&\qquad+\Delta t_n\big(f_2(u(\cdot,t_n),v(\cdot,t_n))-f_2(U^n,V^n),w\big)+\Delta t_n(\mathcal{T}_2^n,w),\quad \forall w\in\mathcal{V}_2^n. &(2.14b)
\end{aligned}$$

Using (2.9a) and (2.9b), we derive that

$$(e_1^{j-1}-\tilde{e}_1^{j-1},w)=(\widetilde{U}^{j-1}-U^{j-1},w)=0, \qquad \forall w\in\mathcal{V}_1^j, \quad j=1,\cdots,n, \tag{2.15a}$$

$$(e_2^{j-1}-\tilde{e}_2^{j-1},w)=(\widetilde{V}^{j-1}-V^{j-1},w)=0, \qquad \forall w\in\mathcal{V}_2^j, \quad j=1,\cdots,n. \tag{2.15b}$$

Therefore, choosing $w=\sigma_1^n$ in (2.14a) and $w=\sigma_2^n$ in (2.14b) gives that

$$\begin{aligned}&(\sigma_1^n,\sigma_1^n)+\mathscr{D}_1\Delta t_n B_1(\sigma_1^n,\sigma_1^n)\\&=(\epsilon_1^n-\epsilon_1^{n-1},\sigma_1^n)+(\sigma_1^{n-1},\sigma_1^n)\\&\qquad+\Delta t_n(f_1(u(\cdot,t_n),v(\cdot,t_n))-f_1(U^n,V^n),\sigma_1^n)+\Delta t_n(\mathcal{T}_1^n,\sigma_1^n),\end{aligned} \tag{2.16a}$$

$$\begin{aligned}&(\sigma_2^n,\sigma_2^n)+\mathscr{D}_2\Delta t_n B_2(\sigma_2^n,\sigma_2^n)\\&=(\epsilon_2^n-\epsilon_2^{n-1},\sigma_2^n)+(\sigma_2^{n-1},\sigma_2^n)\\&\qquad+\Delta t_n(f_2(u(\cdot,t_n),v(\cdot,t_n))-f_2(U^n,V^n),\sigma_2^n)+\Delta t_n(\mathcal{T}_2^n,\sigma_2^n).\end{aligned} \tag{2.16b}$$

Using Cauchy-Schwartz inequality, conditions (1.2) and triangle inequality, we obtain that

$$\begin{aligned}&|(f_1(u(\cdot,t_n),v(\cdot,t_n))-f_1(U^n,V^n),\sigma_1^n)|\\&\le\|f_1(u(\cdot,t_n),v(\cdot,t_n))-f_1(U^n,V^n)\|_{L^2(\Omega)}\|\sigma_1^n\|_{L^2(\Omega)}\\&\le L\|(u(\cdot,t_n)-U^n)+(v(\cdot,t_n)-V^n)\|_{L^2(\Omega)}\|\sigma_1^n\|_{L^2(\Omega)}\\&\le L\Big[\|(u(\cdot,t_n)-U^n)\|_{L^2(\Omega)}+\|(v(\cdot,t_n)-V^n)\|_{L^2(\Omega)}\Big]\|\sigma_1^n\|_{L^2(\Omega)}\\&\le L\Big[\|\sigma_1^n\|_{L^2(\Omega)}+\|\epsilon_1^n\|_{L^2(\Omega)}+\|\sigma_2^n\|_{L^2(\Omega)}+\|\epsilon_2^n\|_{L^2(\Omega)}\Big]\|\sigma_1^n\|_{L^2(\Omega)},\end{aligned} \tag{2.17}$$

and similarly

$$\begin{aligned}&|(f_2(u(\cdot,t_n),v(\cdot,t_n))-f_2(U^n,V^n),\sigma_2^n)|\\&\le L\Big[\|\sigma_1^n\|_{L^2(\Omega)}+\|\epsilon_1^n\|_{L^2(\Omega)}+\|\sigma_2^n\|_{L^2(\Omega)}+\|\epsilon_2^n\|_{L^2(\Omega)}\Big]\|\sigma_2^n\|_{L^2(\Omega)}.\end{aligned} \tag{2.18}$$

Consequently, using (2.17), (2.18), (2.6a) and Cauchy-Schwartz inequality, we derive from (2.16a) and (2.16b) that

$$\begin{aligned}&(1-L\Delta t_n)\|\sigma_1^n\|_{L^2(\Omega)}\\&\le\|\epsilon_1^n-\epsilon_1^{n-1}\|_{L^2(\Omega)}+\|\sigma_1^{n-1}\|_{L^2(\Omega)}\\&\qquad+L\Delta t_n\Big[\|\epsilon_1^n\|_{L^2(\Omega)}+\|\sigma_2^n\|_{L^2(\Omega)}+\|\epsilon_2^n\|_{L^2(\Omega)}\Big]+\Delta t_n\|\mathcal{T}_1^n\|_{L^2(\Omega)},\end{aligned} \tag{2.19a}$$

$$\begin{aligned}&(1-L\Delta t_n)\|\sigma_2^n\|_{L^2(\Omega)}\\&\le\|\epsilon_2^n-\epsilon_2^{n-1}\|_{L^2(\Omega)}+\|\sigma_2^{n-1}\|_{L^2(\Omega)}\\&\qquad+L\Delta t_n\Big[\|\sigma_1^n\|_{L^2(\Omega)}+\|\epsilon_1^n\|_{L^2(\Omega)}+\|\epsilon_2^n\|_{L^2(\Omega)}\Big]+\Delta t_n\|\mathcal{T}_2^n\|_{L^2(\Omega)}.\end{aligned} \tag{2.19b}$$

Denote

$$A_n := \|\epsilon_1^n - \epsilon_1^{n-1}\|_{L^2(\Omega)} + \Delta t_n \|\mathcal{T}_1^n\|_{L^2(\Omega)} + L\Delta t_n [\|\epsilon_1^n\|_{L^2(\Omega)} + \|\epsilon_2^n\|_{L^2(\Omega)}], \tag{2.20a}$$

$$B_n := \|\epsilon_2^n - \epsilon_2^{n-1}\|_{L^2(\Omega)} + \Delta t_n \|\mathcal{T}_2^n\|_{L^2(\Omega)} + L\Delta t_n [\|\epsilon_1^n\|_{L^2(\Omega)} + \|\epsilon_2^n\|_{L^2(\Omega)}]. \tag{2.20b}$$

Then adding together inequalities (2.19a) and (2.19b) gives that

$$\begin{aligned}
&(1-2L\Delta t_n)[\|\sigma_1^n\|_{L^2(\Omega)} + \|\sigma_2^n\|_{L^2(\Omega)}] \\
\le& [\|\sigma_1^{n-1}\|_{L^2(\Omega)} + \|\sigma_2^{n-1}\|_{L^2(\Omega)}] + (A_n + B_n) \\
\le& (1+2L\Delta t_n)\left[\|\sigma_1^{n-1}\|_{L^2(\Omega)} + \|\sigma_2^{n-1}\|_{L^2(\Omega)}\right] + \Delta t_n \frac{A_n + B_n}{\Delta t_n}.
\end{aligned} \tag{2.21}$$

Applying Lemma 2.1 (Gronwall-inequality) to (2.21) gives that

$$\max_{0\le n\le m} \left[\|\sigma_1^n\|_{L^2(\Omega)} + \|\sigma_2^n\|_{L^2(\Omega)}\right] \lesssim \left[\|\sigma_1^0\|_{L^2(\Omega)} + \|\sigma_2^0\|_{L^2(\Omega)}\right] + \sum_{n=1}^{m} (A_n + B_n). \tag{2.22}$$

Since

$$\begin{aligned}
&(U^0, w) = (\varphi, w) = (u(x,0), w), \quad w \in \mathcal{V}_1^n \quad \text{(see (2.7c), (2.8c))}, \\
&(V^0, w) = (\psi, w) = (v(x,0), w), \quad w \in \mathcal{V}_2^n \quad \text{(see (2.7d), (2.8d))},
\end{aligned}$$

we have, for $i=1,2$,

$$\sigma_i^0 - \epsilon_i^0 = e_i^0 \equiv 0,$$

and thus $\sigma_i^0 = \epsilon_i^0$. Therefore it follows from (2.11) that

$$\begin{aligned}
&\|\sigma_1^0\|_{L^2(\Omega)} + \|\sigma_2^0\|_{L^2(\Omega)} \\
\le& \|\epsilon_1^0\|_{L^2(\Omega)} + \|\epsilon_2^0\|_{L^2(\Omega)} \\
\lesssim& \left[N^{-\gamma_1}\|\varphi\|_{H^{\gamma_1}(\Omega)} + N^{-\gamma_2}\|\psi\|_{H^{\gamma_2}(\Omega)}\right].
\end{aligned} \tag{2.23}$$

Moreover from (2.11), we estimate that

$$\|\epsilon_1^n\|_{L^2(\Omega)} + \|\epsilon_2^n\|_{L^2(\Omega)} \lesssim \left[N^{-\gamma_1}\|u\|_{H^{\gamma_1}(\Omega)} + N^{-\gamma_2}\|v\|_{H^{\gamma_2}(\Omega)}\right]. \tag{2.24}$$

Using

$$\epsilon_1^n - \epsilon_1^{n-1} = [R_n^1(u(\cdot,t_n) - u(\cdot,t_{n-1})) - (u(\cdot,t_n) - u(\cdot,t_{n-1}))] + (R_n^1 - R_{n-1}^1) u(\cdot,t_{n-1}),$$

we have

$$\begin{aligned}
&\|\epsilon_1^n - \epsilon_1^{n-1}\|_{L^2(\Omega)} \\
\le& \|R_n^1(u(\cdot,t_n) - u(\cdot,t_{n-1})) - (u(\cdot,t_n) - u(\cdot,t_{n-1}))\|_{L^2(\Omega)} \\
&+ \|(R_n^1 - R_{n-1}^1) u(\cdot,t_{n-1})\|_{L^2(\Omega)}.
\end{aligned} \tag{2.25}$$

Using (2.11) we estimate

$$\begin{aligned}
&\|R_n^1(u(\cdot,t_n)-u(\cdot,t_{n-1}))-(u(\cdot,t_n)-u(\cdot,t_{n-1}))\|_{L^2(\Omega)} \\
\lesssim& N^{-\gamma_1}\Big\|\int_{t_{n-1}}^{t_n} u_t dt\Big\|_{H^{\gamma_1}(\Omega)} \\
\lesssim& N^{-\gamma_1}\int_{t_{n-1}}^{t_n}\|u_t\|_{H^{\gamma_1}(\Omega)}dt,
\end{aligned} \tag{2.26}$$

and

$$\begin{aligned}
&\|(R_n^1-R_{n-1}^1)u(\cdot,t_{n-1})\|_{L^2(\Omega)} \\
\le&\|u(\cdot,t_{n-1})-R_n^1u(\cdot,t_{n-1})\|_{L^2(\Omega)}+\|u(\cdot,t_{n-1})-R_{n-1}^1u(\cdot,t_{n-1})\|_{L^2(\Omega)} \\
\lesssim& N^{-\gamma_1}\|u(\cdot,t_{n-1})\|_{H^{\gamma_1}(\Omega)}.
\end{aligned} \tag{2.27}$$

Therefore combining (2.26) and (2.27) with (2.25) gives that

$$\|\epsilon_1^n-\epsilon_1^{n-1}\|_{L^2(\Omega)}\lesssim N^{-\gamma_1}\int_{t_{n-1}}^{t_n}\|u_t\|_{H^{\gamma_1}(\Omega)}dt+N^{-\gamma_1}\|u(\cdot,t_{n-1})\|_{H^{\gamma_1}(\Omega)}. \tag{2.28}$$

Similarly we can obtain that

$$\|\epsilon_2^n-\epsilon_2^{n-1}\|_{L^2(\Omega)}\lesssim N^{-\gamma_2}\int_{t_{n-1}}^{t_n}\|v_t\|_{H^{\gamma_2}(\Omega)}dt+N^{-\gamma_2}\|v(\cdot,t_{n-1})\|_{H^{\gamma_2}(\Omega)}. \tag{2.29}$$

Furthermore using Taylor's theorem we can estimate that

$$\|\mathcal{T}_1^n\|_{L^2(\Omega)}\lesssim\Delta t_n\|u_{tt}(\cdot,t_n)\|_{L^2(\Omega)},\quad \|\mathcal{T}_2^n\|_{L^2(\Omega)}\lesssim\Delta t_n\|v_{tt}(\cdot,t_n)\|_{L^2(\Omega)}. \tag{2.30}$$

Consequently using (2.24), (2.28), (2.29) and (2.30), we obtain that

$$\begin{aligned}
\sum_{n=1}^m(A_n+B_n)\lesssim& N^{-\gamma_1}\Big[\|u\|_{H^{\gamma_1}(\Omega)}+\int_0^{t_m}\|u_t\|_{H^{\gamma_1}(\Omega)}dt+\sum_{n=1}^{m+1}\|u(\cdot,t_{n-1})\|_{H^{\gamma_1}(\Omega)}\Big] \\
&+N^{-\gamma_2}\Big[\|v\|_{H^{\gamma_2}(\Omega)}+\int_0^{t_m}\|v_t\|_{H^{\gamma_2}(\Omega)}dt+\sum_{n=1}^{m+1}\|v(\cdot,t_{n-1})\|_{H^{\gamma_2}(\Omega)}\Big] \\
&+\tau_m\sum_{n=1}^m\Delta t_n\big[\|u_{tt}(\cdot,t_n)\|_{L^2(\Omega)}+\|v_{tt}(\cdot,t_n)\|_{L^2(\Omega)}\big].
\end{aligned} \tag{2.31}$$

Finally incorporating (2.24), (2.22), (2.23) and (2.31) into the following inequality

$$\|e_1^m\|_{L^2(\Omega)}+\|e_2^m\|_{L^2(\Omega)}\le\|\epsilon_1^m\|_{L^2(\Omega)}+\|\epsilon_2^m\|_{L^2(\Omega)}+\|\sigma_1^m\|_{L^2(\Omega)}+\|\sigma_2^m\|_{L^2(\Omega)}$$

completes the proof of this theorem. $\square$

3 Numerical examples and applications

In this section, we shall implement moving finite element methods (2.8c)-(2.8d) for the proposed problem (1.1a)-(1.1d) to verify the convergence rates and apply to the predator-prey models. To this end, we propose the following iteration algorithm to solve a system of nonlinear algebraic equations arising in moving finite element methods (2.8c)-(2.8d).

Algorithm 1 (Iteration Algorithm for Nonlinear Equations)**.** Solve the nonlinear equations at time level t_n as follows:

1. Set starting values for iterations $[U^n]^{(0)}=\widetilde{U}^{n-1}$ and $[V^n]^{(0)}=\widetilde{V}^{n-1}$, where $\widetilde{U}^{n-1}$ and $\widetilde{V}^{n-1}$ are the projections defined by (2.9a) and (2.9b).
2. Set $\ell=0$ and small value of the error tolerance Tol.
   for $i=0,1,\cdots,$
   solve the following linearized problem

$$\begin{aligned}&\Big(\frac{[U^n]^{(i+1)}-\widetilde{U}^{n-1}}{\Delta t_n},w\Big)+\mathscr{D}_1B_1([U^n]^{(i+1)},w)\\&=(f_1([U^n]^{(i)},[V^n])]^{(i)},w)+(h_1(x,t_n),w),\qquad \forall w\in\mathcal{V}_1^n,\\&\Big(\frac{[V^n]^{(i+1)}-\widetilde{V}^{n-1}}{\Delta t_n},w\Big)+\mathscr{D}_2B_2([V^n]^{(i+1)},w)\\&=(f_2([U^n]^{(i)},[V^n])]^{(i)},w)+(h_2(x,t_n),w),\qquad \forall w\in\mathcal{V}_2^n.\end{aligned}$$

   if $\|[U^n]^{(i+1)}-[U^n]^{(i)}\|_{L^2(\Omega)}<Tol$ and $\|[V^n]^{(i+1)}-[V^n]^{(i)}\|_{L^2(\Omega)}<Tol$
   $\ell=i+1$; break;
   end
3. Output $U^n=[U^n]^{(\ell)}$ and $V^n=[V^n]^{(\ell)}$.

We use the first two examples to verify the convergence rates of finite element methods (2.8a)-(2.8d) for (1.1a)-(1.1d).

In the following computations, the temporal meshes are taken as $t_n=nT/M$, $n=0,1,\cdots,M$ and the space nodes are generated by de Boor's moving mesh algorithm (see e.g., [20,34]). The moving mesh monitor functions are taken as

$$\rho(x,t)=\Big\{1+\frac{\theta}{2}\Big[\Big(\frac{\partial u}{\partial x}\Big)^2+\Big(\frac{\partial v}{\partial x}\Big)^2\Big]+\frac{1-\theta}{2}\Big[\Big(\frac{\partial^2 u}{\partial x^2}\Big)^2+\Big(\frac{\partial^2 v}{\partial x^2}\Big)^2\Big]\Big\}^{\mu},$$

where parameters $0\le\theta\le1$ and $\mu\ge0$ are adjusted to generate good moving meshes, $\mu=0$ represents fixed mesh and $\mu>0$ moving mesh. We use the central difference methods to discretize the first and second order derivatives involved in $\rho(x,t)$ and use uniform spatial meshes at the initial time level in the computations.

The rates of the convergence are computed by the following formula

$$\text{Rate for space} = \frac{\log(\|\text{Error on finer grid}\|_{L^2(\Omega)} / \|\text{Error on coarse grid}\|_{L^2(\Omega)})}{\log(\text{Number of finer grid}/\text{Number of coarse grid})},$$
$$\text{Rate for time} = \frac{\log(\|\text{Error on finer grid}\|_{L^2(\Omega)} / \|\text{Error on coarse grid}\|_{L^2(\Omega)})}{\log(\text{Number of finer grid}/\text{Number of coarse grid})}.$$

The iteration algorithm is applied to solve the nonlinear FEM equations with $\text{Tol}=10^{-16}$.

Example 3.1. In order to estimate the convergence rates, we construct an analytic solution to the model (1.1a)-(1.1b) for $x\in\Omega:=(0,1)$ as follows

$$u(x,t)=(t^\sigma+c)x^{m_1}(1-x)^{n_1}, \tag{3.1a}$$
$$v(x,t)=(t^\sigma+c)x^{m_2}(1-x)^{n_2}, \tag{3.1b}$$

where $\sigma\geq 1$, $c\geq 0$, and m_i, $n_i\in\mathbb{Z}$ and $m_i\geq 2$, $n_i\geq 2$, $i=1,2$. Functions $h_i(x,t)$, $i=1,2$ in (1.1a)-(1.1b) are given by

$$\begin{aligned} h_i(x,t)=&\sigma t^{\sigma-1}x^{m_i}(1-x)^{n_i}-p\xi_1(x,t;2-\beta_i,m_i,n_i)\\ &-q\xi_2(x,t;2-\beta_i,m_i,n_i)-f_i(\eta(x,t;m_1,n_1),\eta(x,t;m_2,n_2)), \end{aligned}$$

where

$$\begin{aligned} &\xi_1(x,t;\beta,m,n)=(t^\sigma+c)\sum_{j=0}^{n}C_n^j(-1)^j\frac{\Gamma(1+m+j)}{\Gamma(1+m+j-\beta)}x^{m+j-\beta},\\ &\xi_2(x,t;\beta,m,n)=(t^\sigma+c)\sum_{j=0}^{n}C_n^j(-1)^j\frac{\Gamma(m+j+1)}{\Gamma(m+j-1)}F(x;2-\beta,m+j-2),\\ &F(x;\beta,k)={}_xD_1^{-\beta}x^k=\sum_{i=0}^{k}\frac{(-1)^i k!(1-x)^{\beta+i}}{(k-i)!\Gamma(1+\beta+i)},\\ &\eta(x,t;m,n)=(t^\sigma+c)x^m(1-x)^n, \end{aligned}$$

and functions $f_i(u,v)$ $(i=1,2)$ are taken as (1.4a) and (1.4b) for Lotka-Volterra model, or as (1.5a) and (1.5b) for Michaelis-Menten-Holling model.

For Lotka-Volterra model (1.4a)-(1.4b), we take the parameters as

$$\mathscr{D}_i=K_i=r_i=1=a_{ij}=1,\quad i,j=1,2.$$

The parameters in (3.1a) and (3.1b) are taken as

$$\sigma=2,\quad m_1=8,\quad m_2=6,\quad n_1=n_2=4.$$

Table 1 illustrates the convergence rates of the finite element methods on uniform spatial meshes with $N+1$ mesh nodes for different values of p, q and β_i.

Table 1: Convergence rates for Example 3.1 for Lotka-Volterra model with different p,q and β_i, $i=1,2$.

Rates in space					Rates in time				
($T=0.01$, $c=1000$, $M=40$)					($T=1$, $c=0$, $N=32$)				
N	Err of u	Rate	Err of v	Rate	M	Err of u	Rate	Err of v	Rate
$p=1$, $q=0$, $\beta_1=0.8$, $\beta_2=0.9$									
8	2.1613e-4	3.5788	2.5587e-4	3.3490	8	1.3195e-5	0.9661	3.5333e-5	0.9703
16	1.8087e-5	3.4137	2.5111e-5	3.7172	16	6.7544e-6	0.9776	1.8033e-5	0.9831
24	4.5316e-6	3.6703	5.5627e-6	3.9385	24	4.5439e-6	0.9806	1.2104e-5	0.9870
32	1.5764e-6	3.7543	1.7914e-6	3.9895	32	3.4269e-6	0.9811	9.1126e-6	0.9885
40	6.8211e-7	3.8114	7.3549e-7	3.9534	40	2.7531e-6	0.9805	7.3088e-6	0.9889
48	3.4045e-7	3.8219	3.5771e-7	3.9072	48	2.3024e-6	0.9794	6.1029e-6	0.9889
56	1.8888e-7	3.8022	1.9586e-7	3.9085	56	1.9797e-6	0.9780	5.2399e-6	0.9886
64	1.1368e-7	—	1.1622e-7	—	64	1.7373e-6	—	4.5919e-6	—
$p=0.5$, $q=0.5$, $\beta_1=0.1$, $\beta_2=0.2$									
8	1.7780e-4	3.7311	2.2556e-4	3.6212	8	3.1720e-6	0.9954	1.0304e-5	0.9938
16	1.3389e-5	3.6591	1.8330e-5	3.8432	16	1.5910e-6	0.9980	5.1743e-6	0.9973
24	3.0368e-6	3.8283	3.8585e-6	3.9278	24	1.0615e-6	0.9987	3.4533e-6	0.9982
32	1.0095e-6	3.8996	1.2464e-6	3.9604	32	7.9641e-7	0.9990	2.5912e-6	0.9987
40	4.2286e-7	3.9347	5.1507e-7	3.9751	40	6.3726e-7	0.9991	2.0736e-6	0.9989
48	2.0636e-7	3.9477	2.4952e-7	3.9674	48	5.3113e-7	0.9992	1.7283e-6	0.9991
56	1.1229e-7	3.9701	1.3536e-7	3.9957	56	4.5530e-7	0.9993	1.4816e-6	0.9992
64	6.6087e-8	—	7.9391e-8	—	64	3.9843e-7	—	1.2965e-6	—
$p=0$, $q=1$, $\beta_1=0.8$, $\beta_2=0.2$									
8	1.8694e-4	3.5526	2.5525e-4	3.6038	8	9.0860e-6	0.9828	1.0587e-5	0.9932
16	1.5931e-5	3.8356	2.0993e-5	4.0560	16	4.5972e-6	0.9907	5.3183e-6	0.9969
24	3.3637e-6	4.0272	4.0536e-6	4.0978	24	3.0763e-6	0.9936	3.5498e-6	0.9981
32	1.0560e-6	4.0786	1.2470e-6	4.0546	32	2.3115e-6	0.9951	2.6638e-6	0.9986
40	4.2501e-7	4.0788	5.0458e-7	3.9097	40	1.8512e-6	0.9960	2.1317e-6	0.9989
48	2.0203e-7	3.9724	2.4737e-7	3.8998	48	1.5437e-6	0.9966	1.7767e-6	0.9991
56	1.0951e-7	3.8317	1.3560e-7	3.6375	56	1.3239e-6	0.9971	1.5231e-6	0.9992
64	6.5657e-8	—	8.3430e-8	—	64	1.1588e-6	—	1.3329e-6	—

For Michaelis-Menten-Holling model (1.5a)-(1.5b), we take

$$Q(v)=\frac{\gamma+\delta v}{1+v},$$

and

$$\gamma=0.1,\quad \delta=0.2,\quad r=0.1,\quad d_1=d_2=0.1,\quad K=10,\quad \kappa=10,\quad \beta_1=0.8,\quad \beta_2=0.2.$$

Table 2 gives the convergence rates of the finite element methods on uniform meshes.

We can see from both Table 1 and Table 2 that the convergence rates are about 4 in space and 1 in time.

Table 2: Convergence rates for Example 3.1 for Michaelis-Menten-Holling model.

$p=0.5$, $q=0.5$, $\beta_1=0.8$, $\beta_2=0.2$									
Rates in space ($T=0.01$, $c=1000$, $M=40$)					Rates in time ($T=1$, $c=0$, $N=32$)				
N	Err of u	Rate	Err of v	Rate	M	Err of u	Rate	Err of v	Rate
8	1.7339e-4	3.7944	2.2557e-4	3.6212	8	1.6025e-5	0.9769	9.7194e-6	0.9946
16	1.2496e-5	3.7106	1.8331e-5	3.8431	16	8.1419e-6	0.9866	4.8776e-6	0.9977
24	2.7756e-6	3.8834	3.8586e-6	3.9278	24	5.4574e-6	0.9905	3.2547e-6	0.9985
32	9.0815e-7	3.9553	1.2465e-6	3.9604	32	4.1043e-6	0.9926	2.4420e-6	0.9989
40	3.7570e-7	3.9894	5.1509e-7	3.9751	40	3.2888e-6	0.9939	1.9541e-6	0.9991
48	1.8153e-7	3.9782	2.4953e-7	3.9672	48	2.7437e-6	0.9948	1.6287e-6	0.9992
56	9.8315e-8	4.0360	1.3537e-7	3.9960	56	2.3536e-6	0.9955	1.3962e-6	0.9992
64	5.7354e-8	—	7.9394e-8	—	64	2.0606e-6	—	1.2217e-6	—

Example 3.2. Let $m_i \in \mathbb{Z}$ and $m_i \geq 2$,

$$\begin{aligned}
&\eta(x,t;m,\lambda)=\begin{cases} x^{\lambda t+m}, & 0\leq x\leq 1/2, \\ x^{\lambda t+m}-(2x-1)^{\lambda t+m}, & 1/2<x\leq 1, \end{cases} \\
&g_1(x,t;m,\lambda,\alpha)=x^{\lambda t+m}\Big[\lambda\log x-\frac{\Gamma(1+\lambda t+m)x^{-\alpha}}{\Gamma(1+\lambda t+m-\alpha)}\Big], \\
&g_2(x,t;m,\lambda,\alpha)=(2x-1)^{\lambda t+m}\Big[\lambda\log(2x-1)-\frac{\Gamma(1+\lambda t+m)(x-1/2)^{-\alpha}}{\Gamma(1+\lambda t+m-\alpha)}\Big], \\
&\xi(x,t;m,\lambda,\alpha)=\begin{cases} g_1(x,t;m,\lambda,\alpha), & 0\leq x\leq 1/2, \\ g_1(x,t;m,\lambda,\alpha)-g_2(x,t,m,\lambda,\alpha), & 1/2<x\leq 1, \end{cases}
\end{aligned}$$

and $f_i(u,v)$ be defined by (1.4a) and (1.4b) for Lotka-Volterra model, or defined by (1.5a) and (1.5b) for Michaelis-Menten-Holling model, and

$$h_i(x,t)=\xi(x,t;m_i,\lambda_i,2-\beta_i)-f_i(\eta(x,t;m_1,\lambda_1),\eta(x,t;m_2,\lambda_2)).$$

Then we can verify that

$$u(x,t)=\eta(x,t;m_1,\lambda_1), \quad v(x,t)=\eta(x,t;m_2,\lambda_2),$$

are the solutions to the model (1.1a)-(1.1b) with $p=1$, $q=0$ for $x\in\Omega:=(0,1)$.

We draw the exact solution in Fig. 1 which shows that the solution has developing singularity. Therefore, this is a good example to compare the performance of fixed meshes and moving meshes for the finite element methods.

Table 3 and Table 4 give the errors and convergence rates of the finite element methods on fixed and moving meshes. The results show that both the moving mesh methods and fixed mesh methods have convergence rate 1 in time and about 4 in space. Moreover, the error for moving meshes is smaller than that for fixed meshes.

Table 3: Convergence rate in time for Example 3.2 for Lotka-Volterra model.

$\beta_1=0.8$, $\beta_2=0.9$, $T=1$, $m_1=7$, $m_2=8$, $\lambda_1=12$, $\lambda_2=10$, $r_i=0.1$, $\mathscr{D}_i=1$								
	Fixed mesh ($N=64$)				Moving mesh ($\theta=0.9$, $\mu=0.01$, $N=16$)			
M	Err of u	Rate	Err of v	Rate	Err of u	Rate	Err of v	Rate
8	1.4713e-3	1.0322	1.3032e-3	1.0122	1.4578e-3	1.0491	1.3083e-3	1.0402
16	7.1941e-4	1.0365	6.4610e-4	1.0280	7.0449e-4	1.0550	6.3621e-4	1.0469
24	4.7255e-4	1.0384	4.2585e-4	1.0325	4.5929e-4	1.0610	4.1613e-4	1.0721
32	3.5051e-4	1.0411	3.1642e-4	1.0353	3.3847e-4	1.0515	3.0569e-4	1.0478
40	2.7784e-4	1.0444	2.5115e-4	1.0379	2.6768e-4	1.0828	2.4196e-4	1.1130
48	2.2967e-4	1.0479	2.0784e-4	1.0405	2.1972e-4	1.0672	1.9751e-4	1.0576
56	1.9541e-4	1.0514	1.7704e-4	1.0431	1.8639e-4	1.0849	1.6780e-4	1.1059
64	1.6981e-4	—	1.5402e-4	—	1.6125e-4	—	1.4476e-4	—

Table 4: Convergence rate in space for Example 3.2 for Lotka-Volterra model.

$\beta_1=0.8$, $\beta_2=0.9$, $T=1$, $m_1=7$, $m_2=8$, $\lambda_1=12$, $\lambda_2=10$, $r_i=0.1$, $\mathscr{D}_i=1$.								
	Fixed mesh ($M=500$)				Moving mesh ($M=500$, $\theta=0.9$, $\mu=0.01$)			
N	Err of u	Rate	Err of v	Rate	Err of u	Rate	Err of v	Rate
8	2.6411e-2	2.7944	2.7095e-2	2.9162	2.2435e-2	3.1471	2.2793e-2	3.2865
12	8.5055e-3	3.2228	8.3058e-3	3.3379	6.2625e-3	3.5435	6.0127e-3	3.6801
16	3.3655e-3	3.4682	3.1793e-3	3.5681	2.2595e-3	3.7786	2.0858e-3	3.9058
20	1.5522e-3	3.6259	1.4339e-3	3.7107	9.7237e-4	3.9813	8.7249e-4	4.0636
24	8.0140e-4	3.7432	7.2899e-4	3.8145	4.7052e-4	4.0562	4.1591e-4	4.1143
28	4.5004e-4	3.8437	4.0490e-4	3.9025	2.5178e-4	4.0827	2.2057e-4	4.1305
32	2.6936e-4	—	2.4045e-4	—	1.4597e-4	—	1.2706e-4	—

To better compare the performance of uniform mesh and moving mesh, we draw Fig. 2 and Fig. 3 for the exact solutions and computational solutions. These two figures (Fig. 2 and Fig. 3) further show that the moving mesh outperforms fixed mesh in the example.

Example 3.3. For the Michaelis-Menten-Holling predator-prey model (1.5a)-(1.5b), we set $h_i(x,t)=0$ $(i=1,2)$, $u(x,0)=v(x,0)=\sin(\pi x)$, $Q(v)=\frac{\gamma+\delta v}{1+v}$, $\gamma=0.05$, $\delta=0.5$, $r=1$, $d_1=1.1$, $d_2=1$, $K=\kappa=1$, $p=q=0.5$, $\mathscr{D}_1=0.005$, $\mathscr{D}_2=0.05$, $T=30$.

It has much difficulty to study the stability properties of the equilibrium solutions in a fractional diffusion model, we apply our moving mesh FEM to simulate the evolution of the predator and prey. Figs. 4 and 5 give the solutions with various dispersion order β_i, $i=1,2$. We observe that the solutions $u(x,t)$ and $v(x,t)$ tend to be positive nontrivial equilibrium as time approaches to infinity. But the shapes of equilibrium for u and v are very different. Fig. 6 describes different shapes of stable solutions with various β_i, $i=1,2$. Fig. 7 describes different shapes of stable solutions with fixed $d_2=1$ and various d_1.

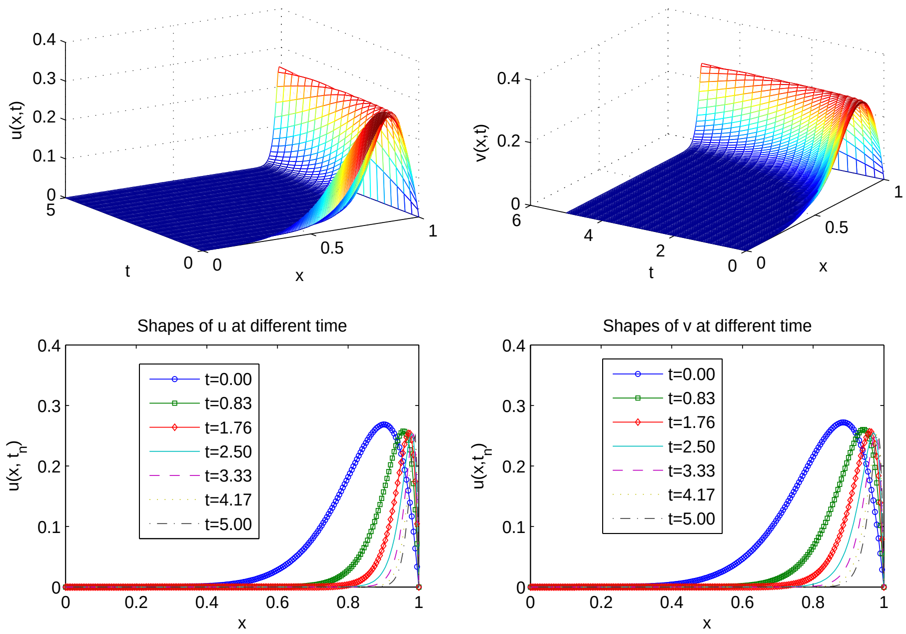

Figure 1: Exact solutions for Example 3.2 with $T=5$, $\lambda_1=12$, $\lambda_2=10$, $m_1=m_2=4$.

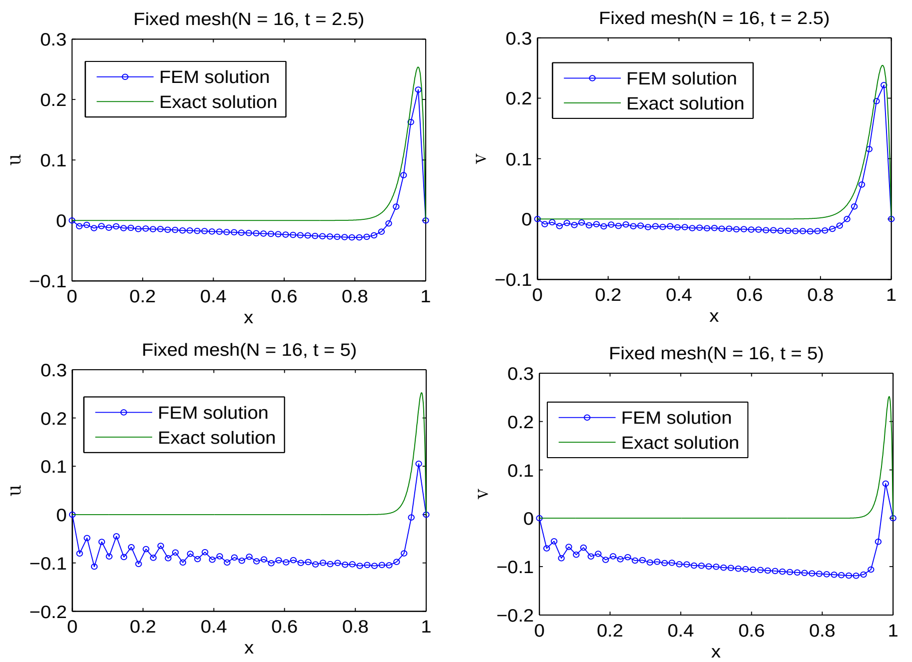

Figure 2: Computational solutions using fixed meshes for Example 3.2 with $\lambda_1=12$, $\lambda_2=10$, $m_1=m_2=4$. Other parameters are taken as in Table 4.

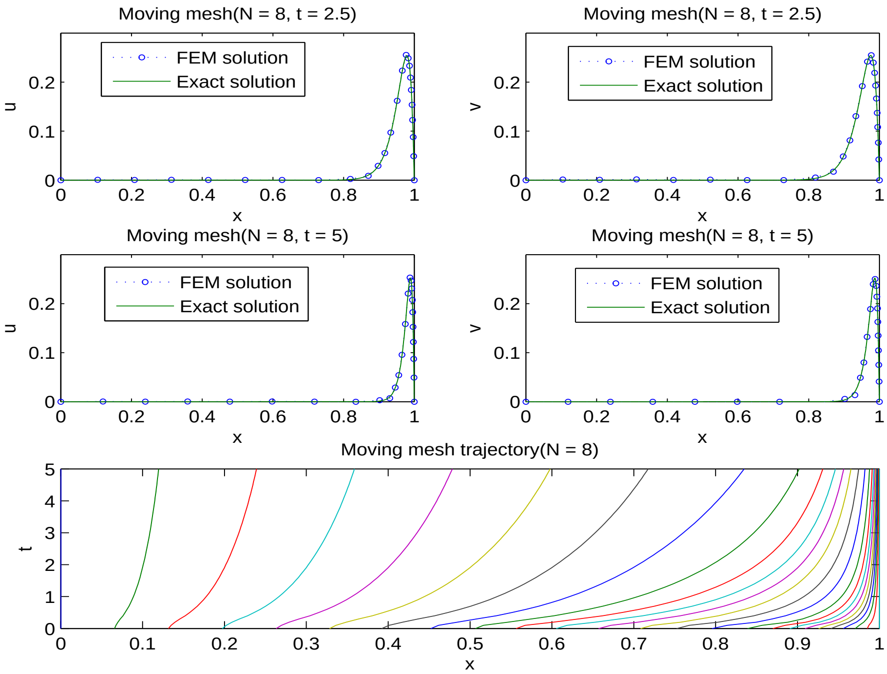

Figure 3: The upper four figures: Computational solutions using moving mesh for Example 3.2 with $\lambda_1=12$, $\lambda_2=10$, $m_1=m_2=4$ and $\theta=0.9$, $\mu=0.05$ in the monitor function. Other parameters are taken as in Table 4. The bottom figure: Moving mesh trajectory.

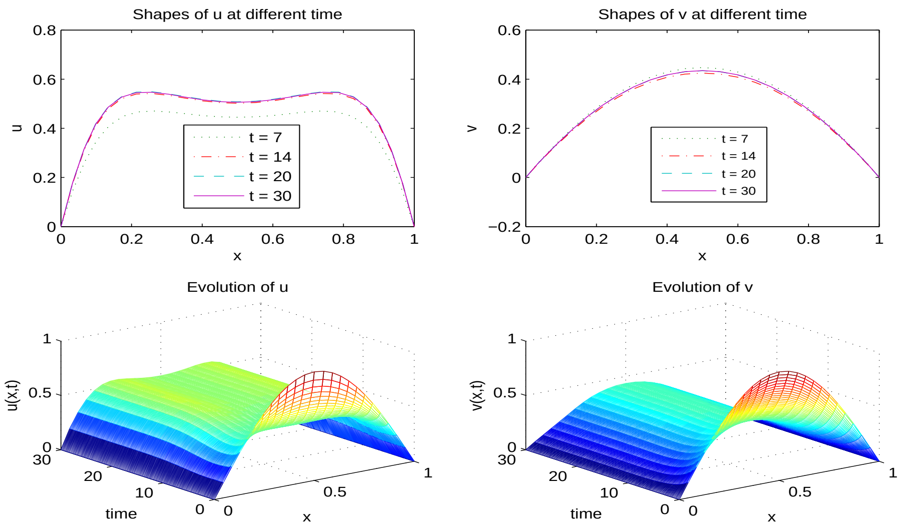

Figure 4: Evolution of solutions for Example 3.3 with $\beta_i=0.1$ and $\mu=0.06$, $\theta=0.9$ in the monitor function. Upper left: Shapes of u at different time. Upper right: Shapes of v at different time. Lower left: Evolution of u from $t=0$ to $t=30$. Lower right: Evolution of v from $t=0$ to $t=30$.

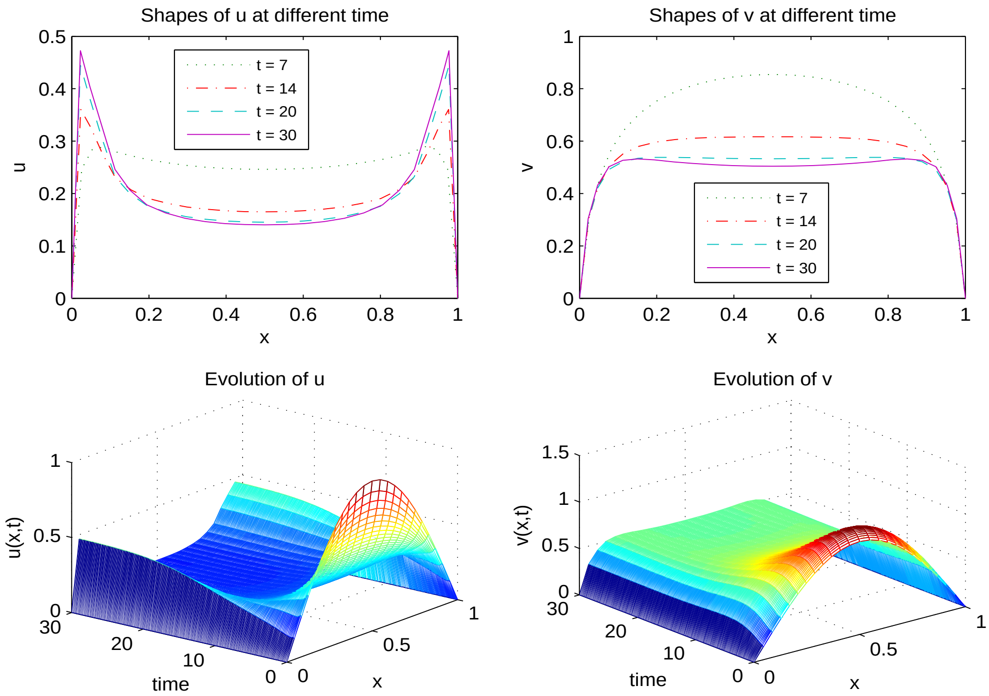

Figure 5: Evolution of solutions for Example 3.3 with $\beta_i = 0.8$ and $\mu = 0.06$, $\theta = 0.9$ in the monitor function. Upper left: Shapes of u at different time. Upper right: Shapes of v at different time. Lower left: Evolution of u from $t=0$ to $t=30$. Lower right: Evolution of v from $t=0$ to $t=30$.

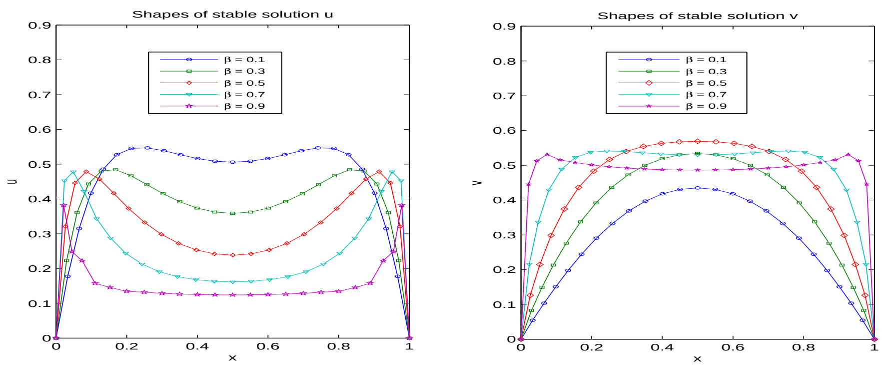

Figure 6: Different shapes of stable solutions with various β_i for Example 3.3 and $\mu = 0.06$, $\theta = 0.9$ in the monitor function.

4 Conclusions

In this paper we studied moving finite element methods for a system of semi-linear fractional diffusion equations which arise in competitive predator-prey models by replacing

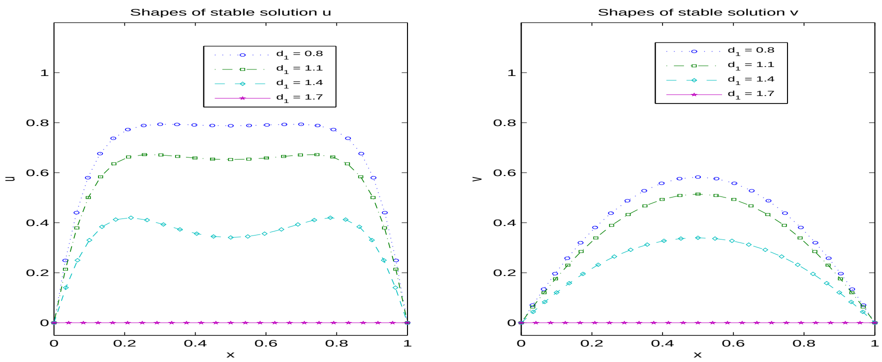

Figure 7: Different shapes of stable solutions with various d_1 for Example 3.3 and $\mu=0.06$, $\theta=0.9$ in the monitor function.

the second-order derivatives in the spatial variables with fractional derivatives of order less than two. The convergence rates of the methods were proved and verified by a variety of numerical examples. Applications in anomalous diffusive Lotka-Volterra and Michaelis-Menten-Holling predator-prey models were also studied.

Acknowledgments

The authors are grateful to Professor Fawang Liu for his helpful suggestions. The work was supported by National Natural Science Foundation of China (Grant No. 11171274).

References

[1] B. BAEUMER, M. KOVÁCS AND M. M. MEERSCHAERT, *Fractional reproduction-dispersal equations and heavy tail dispersal kernels*, Bull. Math. Biol., 69 (2007), pp. 2281–2297.

[2] B. BAEUMER, M. KOVÁCS AND M. M. MEERSCHAERT, *Numerical solutions for fractional reaction-diffusion equations*, Comput. Math. Appl., 55 (2008), pp. 2212–2226.

[3] R. E. BANK AND R. F. SANTOS, *Analysis of some moving space-time finite element methods*, SIAM J. Numer. Anal., 30 (1993), pp. 1–18.

[4] F. BRAUER AND C. CASTILLO-CHAVEZ, Mathematical Models in Population Biology and Epidemiology, Springer-Verlag, Heidelberg, 2000.

[5] M. CAVANI AND M. FARKAS, *Bifurcation in a predator-prey model with memory and diffusion, II: Turing bifurcation*, Acta Math. Hungar., 63 (1994), pp. 375–393.

[6] C. CHEN, F. LIU, V. ANH AND I. TURNER, *Numerical schemes with high spatial accuracy for a variable-order anomalous subdiffusion equation*, SIAM J. Sci. Comput., 32 (2010), pp. 1740–1760.

[7] H. CHEN AND D. XU, *A compact difference scheme for an evolution equation with weakly singular kernel*, Numer. Math. Theor. Meth. Appl., 5 (2012), pp. 559–572.

[8] H. CHEN, D. XU AND Y. PENG, *An alternating direction implicit fractional trapezoidal rule type difference scheme for the two-dimensional fractional evolution equation*, Int. J. Comput. Math., 92 (2015), pp. 2178–2197.

[9] W. Deng, *Finite element method for the space and time fractional Fokker-Planck equation,* SIAM J. Numer. Anal., 47 (2008), pp. 204–226.
[10] W. Deng, S. Du and Y. Wu, *High order finite difference WENO schemes for fractional differential equations,* Appl. Math. Lett., 26 (2013), pp. 362–366.
[11] T. Dupont, *Mesh modification for evolution equations,* Math. Comput., 39 (1982), pp. 85–107.
[12] T. Dupont and Y. Liu, *Symmetric error estimates for moving mesh Galerkin methods for advection-diffusion equations,* SIAM J. Numer. Anal., 40 (2002), pp. 914–927.
[13] V. J. Ervin and J. P. Roop, *Variational formulation for the stationary fractional advection dispersion equation,* Numer. Meth. PDEs, 22 (2006), pp. 558–576.
[14] V. J. Ervin and J. P. Roop, *Variational solution of fractional advection dispersion equations on bounded domains in* $\mathbb{R}^d$, Numer. Meth. PDEs, 23 (2007), pp. 256–281.
[15] V. J. Ervin, N. Heuer and J. P. Roop, *Numerical approximation of a time dependent nonlinear space-fractional diffusion equation,* SIAM J. Numer. Anal., 45 (2007), pp. 572–591.
[16] G. J. Fix and J. P. Roop, *Least squares finite-element solution of a fractional order two-point boundary value problem,* Comput. Math. Appl., 48 (2004), pp. 1017–1033.
[17] N. J. Ford, J. Xiao and Y. Yan, *A finite element method for time fractional partial differential equations,* Fract. Cal. Appl. Anal., 14 (2011), pp. 454–474.
[18] G. Gao and Z. Sun, *A compact finite difference scheme for the fractional sub-diffusion equations,* J. Comput. Phys., 230 (2011), pp. 586–595.
[19] G. Gao, Z. Sun and Y. Zhang, *A finite difference scheme for fractional sub-diffusion equations on an unbounded domain using artificial boundary conditions,* J. Comput. Phys., 231 (2012), pp. 2865–2879.
[20] W. Huang and R. D. Russell, Adaptive Moving Mesh Methods, Springer, New York, 2011.
[21] M. Ilic, F. Liu, I. Turner and V. Anh, *Numerical approximation of a fractional-in-space diffusion equation I,* Frac. Calc. Appl. Anal., 8 (2005), pp. 323–341.
[22] M. Ilic, F. Liu, I. Turner and V. Anh, *Numerical approximation of a fractional-in-space diffusion equation II: with nonhomogeneous boundary conditions,* Frac. Calc. Appl. Anal., 9 (2006), pp. 333–349.
[23] X. Ji and H. Tang, *High-order accurate Runge-Kutta (local) discontinuous Galerkin methods for one- and two-dimensional fractional diffusion equations,* Numer. Math. Theor. Meth. Appl., 5 (2012), pp. 333–358.
[24] Y. Jiang and J. Ma, *High-order finite element methods for time-fractional partial differential equations,* J. Comput. Appl. Math., 235 (2011), pp. 3285–3290.
[25] Y. Jiang and J. Ma, *Moving finite element methods for time fractional partial differential equations,* Sci. China Math., 56 (2013), pp. 1287–1300.
[26] S. Kovács, K. Kiss and M. Farkas, *Qualitative behaviour of a ratio-dependent predator-prey system,* Nonlinear Anal. RWA, 10 (2009), pp. 1627–1642.
[27] X. J. Li and C. J. Xu, *A space-time spectral method for the time fractional diffusion equation,* SIAM J. Numer. Anal., 47 (2009), pp. 2108–2131.
[28] X. J. Li and C. J. Xu, *Existence and uniqueness of the weak solution of the space-time fractional diffusion equation and a spectral method approximation,* Commun. Comput. Phys., 8 (2010), pp. 1016–1051.
[29] J. Ma, *Convergence analysis of moving Godunov methods for dynamical boundary layers,* Comput. Math. Appl., 59 (2010), pp. 80–93.
[30] J. Ma, Y. Jiang and K. Xiang, *On a moving mesh method for solving partial integro-differential equations,* J. Comput. Math., 27 (2009), pp. 713–728.

[31] J. MA AND Y. JIANG, *Analysis of an adaptive remeshing algorithm for reaction-diffusion equations with traveling heat source,* Scientia Sinica Math., 41 (2011), pp. 235–251.

[32] J. MA, W. HUANG AND R. D. RUSSELL, *Analysis of a moving collocation method for one-dimensional partial differential equations,* Sci. China Math., 55 (2012), pp. 827–840.

[33] J. MA AND Y. JIANG, *Moving collocation methods for time fractional differential equations and simulation of blowup,* Sci. China Math., 54 (2011), pp. 611–622.

[34] J. MA, J. LIU AND Z. ZHOU, *Convergence analysis of moving finite element methods for space fractional differential equations,* J. Comput. Appl. Math., 255 (2014), pp. 661–670.

[35] J. A. MACKENZIE AND W. R. MEKWI, *An analysis of stability and convergence of a finite-difference discretization of a model parabolic PDE in 1D using a moving mesh,* IMA J. Numer. Anal., 27 (2007), pp. 507–528.

[36] W. MCLEAN AND K. MUSTAPHA, *Convergence analysis of a discontinuous Galerkin method for a sub-diffusion equation,* Numer. Algorithm, 5 (2009), pp. 69–88.

[37] M. MEERSCHAERT AND C. TADJERAN, *Finite difference approximations for fractional advection dispersion flow equations,* J. Comput. Appl. Math., 172 (2004), pp. 65–77.

[38] M. MEERSCHAERT, H. SCHEFFLER AND C. TADJERAN, *Finite difference methods for two-dimensional fractional dispersion equation,* J. Comput. Phys., 211 (2006), pp. 249–261.

[39] K. MUSTAPHA AND M. MCLEAN, *Piecewise-linear, discontinous Galerkin method for a fractional diffusion equation,* Numer. Algorithm, 56 (2011), pp. 159–184.

[40] J. REN, Z. SUN AND X. ZHAO, *Compact difference scheme for the fractional sub-diffusion equation with Neumann boundary conditions,* J. Comput. Phys., 232 (2013), pp. 456–467.

[41] S. SHEN, F. LIU, V. ANH AND I. TURNER, *The fundemental solution and numerical solution of the Riesz fractional advection-dispersion equation,* IMA J. Appl. Math., 73 (2008), pp. 850–872.

[42] C. TADJERAN, M. MEERSCHAERT AND H. SCHEFFLER, *A second-order accurate numerical approximation for the fractional diffusion equation,* J. Comput. Phys., 213 (2006), pp. 205–213.

[43] C. TADJERAN AND M. MEERSCHAERT, *A second-order accurate numerical method for the two-dimensional fractional diffusion equation,* J. Comput. Phys., 220 (2007), pp. 813–823.

[44] T. TANG AND J. XU, Adaptive Computations: Theory and Algorithms, Science Press, Beijing, 2007.

[45] V. THOMÉE, Galerkin Finite Element Methods for Parabolic Problems, Springer-Verlag, Berlin, 2006.

[46] Q. YANG, F. LIU AND I. TURNER, *Numerical methods for fractional partial differential equations with Riesz space fractional derivatives,* Appl. Math. Model., 34 (2010), pp. 200–218.

[47] Y. YU, W. DENG AND Y. WU, *Positivity and boundedness preserving schemes for the fractional reaction-diffusion equation,* Sci. China Math., 56 (2013), pp. 2161–2178.

[48] X. ZHAO AND Z. SUN, *A box-type scheme for fractional sub-diffusion equation with Neumann boundary conditions,* J. Comput. Phys., 230 (2011), pp. 6061–6074.

[49] H. ZHANG, F. LIU AND V. ANH, *Galerkin finite element approximations of symmetric space-fractional partial differential equations,* Appl. Math. Comput., 217 (2010), pp. 2534–2545.

[50] N. ZHANG, W. DENG AND Y. WU, *Finite difference/element method for a two-dimensional modified fractional diffusion equation,* Adv. Appl. Math. Mech., 4 (2012), pp. 496–518.

[51] Y. ZHANG, Z. SUN AND H. WU, *Error estimate of Crank-Nicolson-type difference for subdiffusion equation,* SIAM J. Numer. Anal., 49 (2011), pp. 2302–2322.

[52] P. ZHUANG, F. LIU, V. ANH AND I. TURNER, *Numerical methods for the variable-order fractional advection-diffusion equation with a nonlinear source term,* SIAM J. Numer. Anal., 47 (2009), pp. 1760–1781.